ISSN: 2472-3703 DOI: 10.6911/WSRJ.202205_8(5).0066

Protective Effect of Flavonoids from Millettia Specisoa Champ on the Apoptosis of Ovarian Granulosa Cells Induced by Cisplatin

Xiaoling Zhang[1], Xuezhen Chen[1], Yuan Huang[1], Xiaohang Wang[1,*] and Chunbin Lu[1]

[1]Department of Developmental and Regenerative Biology, School of Jinan University, Guangzhou 510632, China

[*]tcblu@jnu.edu.cn

Abstract

To determine the protective effect of Flavonoids from Millettia specisoa Champ (FMSC) on cisplatin-induced ovarian granulosa cell damage, mouse ovarian granulosa cells were isolated and cell damage model in vitro was established using 5 μg/mL cisplatin. Cells were divided into a control group, a CDDP group, and FMSC100/200/400 +CDDP group. Cell proliferation was detected by the MTT assay, cell growth was observed using crystal violet, and apoptosis was assessed by TUNEL & Hoechst 33258 staining. qPCR and Western Blot (WB) were performed to respectively measure mRNA and protein expression of proliferation-related molecules (PCNA) and apoptosis-related molecules (Bax and Bcl-2). Results have revealed that cisplatin could damage mouse primary granulosa cells (mGC). After the administration of FMSC, mGC presented improved cell viability and reduced apoptosis levels. qPCR and WB showed increased expression levels of anti-apoptotic gene Bcl-2 and proliferative gene PCNA in mGC. In parallel, the protein expression of the pro-apoptotic gene Bax was reduced in cells treated with FMSC. Therefore, FMSC reduced cisplatin-induced apoptosis in mGC by upregulating the expression of the anti-apoptotic gene Bcl-2. The down-regulation of the expression of the pro-apoptotic gene Bax enhanced the anti-apoptotic ability of FMSC, suggesting that its mechanism of action may be related to apoptosis.

Keywords

Cisplatin; Flavonoids from Millettia specisoa Champ; Ovarian granulosa cells; Apoptosis.

1. INTRODUCTION

Cis-dichlorodiammine Platinum (CDDP), a cytotoxic drug [1], is a widely used antitumor agent. Studies have found that CDDP has therapeutic effects on transplanted tumors [2], tumors induced by viruses or other chemicals, and human tumor xenografts, such as lymphoid leukemia, ovarian cancer, testicular cancer, bladder cancer, head and neck cancer, colorectal and lung cancers [3,4]. It is believed that 40-80% of cancer patients receive chemotherapy involving platinum-based drugs [5]. Meanwhile, the cure rates of cisplatin are as high as 95% for patients with testicular cancer, 42% for head and neck cancer, 41% for cervical cancer, 38% for bladder cancer, and 37% for ovarian cancer [6-10]. The main principle of CDDP exerting its antitumor effects is that it enters the cell since the concentration of chloride ions inside the cell is much lower than that of the extracellular fluid [11, 12]. Cationic hydrate is a strong electrophilic reagent that can react with any nucleophilic reagent [13], such as nucleophilic reactions with sulfhydryl groups present on proteins and nitro donor atoms present on nucleic acids, forming

ISSN: 2472-3703 DOI: 10.6911/WSRJ.202205_8(5).0066

intra- and inter-strand cross-links with DNA to form cisplatin-DNA adducts, which in turn leads to a conformational disorder in the DNA of tumor cells [14, 15]. This process interferes normal DNA replication and transcriptional functions, thus preventing the rapid proliferation of tumor cells, inducing apoptosis, and acting as an anticancer agent [16, 17]. Although cisplatin is widely used, there are side effects to cause damage to normal cells due to poor selectivity of target cell [18,19].

As the most prominent cell population within the ovarian follicle, granulosa cells are a critical component of the ovary, surrounding the oocyte, providing nutrition and participating in follicular developmen and growth [20]. Granulosa cells are the only cells that express follicle-stimulating hormone receptors (FSHR) and are regulated by gonadotropins secreted by the pituitary gland while secreting estradiol and various cytokines themselves [21]. Studies have shown that normal proliferation and differentiation of granulosa cells is crucial in the physiological function of ovarian follicles, including follicular growth and development, maturation, ovulation, luteinization, hormone synthesis and secretion [22]. Therefore, the development and maitaining of functional granulosa cells are essential to reproduction in mammal

Previous studies have shown that low concentrations of cisplatin to induce slight growth inhibition in ovarian granulosa cells cultured in vitro, robust inhibitory effect on granulosa cells were furtherly at high concentrations of cisplatin. The apoptosis of granulosa cells can seriously disrupt the normal physiological function of the ovary and may lead to ovarian damage, which in turn culminates in premature ovarian failure and infertility [23].

In recent years, thealternative theraputic effect of flavonoids on cancer has received increasing attention, and the protective effects of flavonoids on ovarian and granulosa cell damage have been studied. It has been shown that flavonoids can promote the proliferative ability of granulosa cells and inhibit apoptosis [24-26].

Cisplatin as a chemotherapeutic drug for female patients often experience amenorrhea, premature ovarian failure, or even infertility, while flavonoids can promote follicular development, granulosa cell proliferation and inhibit apoptosis. However, there are no reports on whether flavonoids have a protective effect on cisplatin-induced ovarian granulosa cell damage. Therefore, in this study, we have investigated the effects of cisplatin on granulosa cells from mouse ovarian to establish cell model with cisplatin treatment. Intervention with FMSC was performed to investigate the effect of FMSC on damage of ovarian granulosa cells and underlying mechanisms.

2. MATERIALS AND METHODS

2.1. Materials and Reagents

Flavonoids from Millettia specisoa Champ were kindly provided by the Guangdong Academy of Agricultural Sciences Crop Research Institute (Guangdong, China, 2020). cis-Dichlorodiammine Platinum (CDDP) was obtained from Jiangsu Haosen Pharmaceutical Group Co., Ltd.(China). PMSG was obtained from Ningbo No. 2 Hormone Factory (China), DMEN/F2 medium was purchased from Gibco (USA). In situ cell death detection kit was produced by Roche Diagnostics Ltd. (USA). Bcl-2, Bax, β-actin, PCNA, goat anti-rabbit IgG antibody (HRP-conjugated), and horse anti-mouse IgG antibody (HRP-conjugated) were obtained from Cell Signaling Technology (CST, USA). The ECL developer was purchased from Millipore (USA). BCA protein assay kit was obtained from Bioss Ltd. (China). DMSO was obtained from Sigma Ltd. (China) and MTT was obtained from Solarbio Ltd. (China).

ISSN: 2472-3703 DOI: 10.6911/WSRJ.202205_8(5).0066

2.2. Animals

Animals were provided with food and water ad libitum and raised following the national and local guidelines for the care and use of experimental animals. Female Kunming mice (SPF) (21 days old) (animal license: SCXK 2017-0174, Guangdong Experimental Animal Center, China) were placed in an environment-controlled room under 12 h of light and 12h of dark cycle. The temperature was kept at 25 ± 2 °C and humidity at 40%~70%. All experiments were approved under the principles drawn up by the Experimental Animal Ethics Committee.

2.3. Ovarian GC Isolation, Culture, and Treatment

21-day-old female mice were injected with 10 IU PMSG. After 48 h, mice were euthanized, and ovarian GC was isolated as described by Canipari et al. [27] and Wang et al. [28]. The GC was suspended in DMEM / F12 containing 10 % fetal bovine serum, 100 IU/mL penicillin, and 100 μg/mL streptomycin, adjusted to 1 × 106 cells/ml, and cultured continuously at 37 °C and 5 % CO2 for 24 h. Then, the medium was replaced with fresh medium containing 0, 2.5, 5, 7.5 and 10 μg/mL doses of CDDP, and the culture was incubated for 24 hours to observe the effect of cisplatin on the mGCs . Cell damage model was then established with 5 μg/mL cisplatin and intervened with FMSC. GCs were assigned to the following 8 groups: control (CON), cell damage group (CDDP, 5 μg/mL), or cell damage model group treated with FMSC (100, 200, 400, 600, 800 and 1000 μg/ml).

2.4. MTT Assay to Assess Cell Viability

Cells (1×10^5 cells/well) were seeded in a 96-well culture plate and incubated with fresh medium containing the indicated concentrations of CDDP (0, 2.5, 5, 7.5 and 10 μg/mL) or treated with 5 μg/mL CDDP for 24 hours in the presence or absence of FMSC (100, 200, 400, 600, 800 and 1000 μg/mL). Then, 20 μL MTT (5 mg/mL) was added in each well, and cells were incubated at 37 °C for 4 hours. The absorbance was measured in a spectrophotometer at 490 nm.

2.5. Crystalline Violet and Hoechst 33258 Staining for Cell Morphology and Apoptosis

Cells (1×10^6 cells/well) were seeded in a 12-well culture plate and incubated with fresh medium containing the indicated concentrations of CDDP (0, 2.5, 5, 7.5 and 10 μg/mL) or treated with 5 μg/mL CDDP for 24 hours in the presence or absence of FMSC (100, 200 and 400 μg/mL). At the end of the treatment period, the supernatant was discarded and cells washed 3 times with PBS for 5 min each time, followed by the addition of fixative for 20 min at room temperature or overnight at 4 °C. After fixation, cells were washed 3 times with PBS, then 0.1% crystal violet staining solution was added and incubated for 30 min at room temperature, protected from light.

The bisbenzamide dye, Hoechst 33258, was used to detect apoptotic cells. At the end of the treatment period, cells were washed and fixed for Crystalline violet staining. After fixation, slides were immediately stained with 50 g/ml Hoechst 33258 dye diluted in PBS for 10 min in the dark, rinsed with PBS, and allowed to dry in the dark. Finally, the samples were analyzed under an inverted fluorescence microscope to observe apoptotic cell DNA. Cells with intensely fluorescent and/or fragmented nuclei were considered apoptotic.

2.6. Terminal Deoxynucleotidyl Transferase-Mediated Deoxy-uridine Triphosphate Nick-End-Labeling (TUNEL).

Terminal deoxynucleotidyl transferase-mediated DUTP end-labeling (TUNEL) assay was performed using an In Situ Cell Death Detection Kit. First, mGC (1×10^6 cells/well) were plated in 12-well culture plates containing coverslips and treated with 5 μg/mL CDDP for 24 h in the presence or absence of FMSC (100, 200, 400 μg/mL). Then, the supernatant was discarded and

ISSN: 2472-3703 DOI: 10.6911/WSRJ.202205_8(5).0066

cells washed three times with ice-cold PBS for 5 min each, followed by the addition of fixative for 20 min at room temperature or overnight at 4°C. After fixation, the slides were washed 3 times with cold PBS and incubated with the TUNEL reaction mixture for 60 min at 37°C in a humidified atmosphere in the dark. This solution was discarded and cells were washed 3 times with PBS for 5 min each. Finally, the samples were analyzed under an inverted fluorescence microscope to observe the DNA of apoptotic cells (green fluorescence).

2.7. RNA Isolation and Real-time PCR

The mGCs (1×10^6 cells/well) were inoculated in 12-well culture plates containing coverslips and treated with 5 μg/mL CDDP for 24 h in the presence or absence of FMSC (100, 200, 400 μg/mL). Total ribonucleic acid (RNA) extraction from mGCs was performed using RNAiso plus (TaKaRa, China), and the total RNA concentration was determined using a NanoDrop 2000 spectrophotometer (Thermo Fisher Scientific, China). Total RNA from each sample was reverse-transcribed into cDNA and amplified. Forward and reverse primer sequences (5′-3′) were designed as follows: β-actin (F, GGCACCACACCTTCTACAATGAG; R, AGAGGCATACAGGGACAGCAC), Bax (F, GGCCCACCAGCTCTGAAC; R, TTCTTCCAGATGGTGAGCGA), and Bcl-2 (F, GGGGAAACACCAGAATCAAG; R, TCCCTTTGGCAGTAAATAGCT). We performed RT-PCR on a real-time PCR detection system (CFD-3120, Bio-Rad, USA), and the cycle conditions consisted of an initial denaturation of 3 min at 95°C, followed by 40 cycles of 95°C for 5 s, 60°C for 30 s, and 72°C for 15 s. Each experiment was repeated three times and β-actin was used as an internal standard to normalize the relative expression levels of Bax and Bcl-2. The results were given as the mean ± standard deviation, and $2-\Delta\Delta CT$ differences were compared.

2.8. Western Blotting

The mGCs (2×10^6 cells/well) were inoculated in 6-well culture plates and treated with 5 μg/mL CDDP for 24 h in the presence or absence of FMSC (100, 200, 400 μg/mL). At the end of the treatment period, the medium was aspirated, and cells were washed with PBS. Then the cells were digested with 0.25% trypsin for 2 min. After centrifugation of trypsinized cells and growth medium containing detached cells at 300 g for 5 min, cell pellets were washed with PBS, then lysed in ice-cold lysis buffer-RIPA containing a protease inhibitor for 30 min. The lysate was centrifuged at 12000 g for 10 min at 4°C. Then, the supernatants were collected, and the protein levels were determined using the BCA protein assay kit. Proteins were separated by 12% SDS-PAGE and transferred to a PVDF membrane. The membranes were blocked using 5 % fat-free milk for 2 h at room temperature, then incubated with homologous primary antibodies overnight at 4°C. The membranes were then washed and incubated with HRP-conjugated secondary antibody for 1 h at room temperature. The protein was examined using an ECL developer, and the pixel intensity was measured using Image J software.

2.9. Statistical Analysis

Experimental data were presented as mean ± standard deviation of at least three independent experiments. Graphpad Prism 7.0 software was used to analyze the data. One-way ANOVA was used to compare differences among groups. The significance was determined as follows: * $P < 0.05$; ** $P < 0.01$; or *** $P < 0.001$, compared to the control treatment group. Differences were considered to be statistically significant when $P < 0.05$.

3. EXPERIMENTAL RESULTS

3.1. Effect of Different Concentrations of Cisplatin on mGC Cells

3.1.1 Effect of cisplatin on mGC cell viability detected by the MTT assay

ISSN: 2472-3703 DOI: 10.6911/WSRJ.202205_8(5).0066

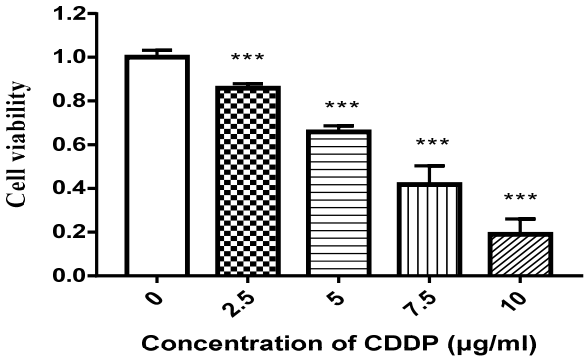

Figure 1. Effect of different concentrations of cisplatin on mGC proliferation.

***P<0.001, compared with the control group.

Table 1. Inhibition rate of mGC cells by different concentrations of cisplatin

CDDP concentration (μg/mL)	Inhibition rate (%)
0	0 ± 3.21
2.5	15.24 ± 3.74 ***
5	34.12 ± 2.78 ***
7.5	70.33 ± 4.24 ***
10	87.63 ± 3.18 ***

As shown in Figure 1. and Table 1, the treatment of 2.5, 5, 7.5, or 10 μg/mL cisplatin significantly inhibited the viability of mGC cells compared with the control in a dose-dependent way. Upon treatment with 10 μg/mL cisplatin for 24 h, the inhibition rate of mGC proliferation reached 87.63%.

3.1.2 Effect of different concentrations of cisplatin on the morphology of mGC cells visualized by crystalline violet

The growth and cell morphology of mGC cells were observed under light microscopy. mGC could be star-shaped or spindle-shaped, with interconnected cellular pseudopods between cells incontrol(Figure 2.A). Crystalline violet staining could be observed with intact cell morphology and clear edges, and the cells were polygonal, star-shaped, or spindle-shaped. The nuclei were stained dark purple and round by crystalline violet, and lavender stained the cytoplasm. The morphology and physiological staus of isolated cells was were as same a cells in the literature, indicating that the isolated cells were primary mGCs. After cisplatin treatment of different concentrations, the growth condition and morphology of mGC were observed. The results showed that the treatment of 2.5, 5, 7.5, and 10 μg/mL cisplatin significantly inhibited the cell viability of mGC compared with the control group, while there were much fewer cells as the high concentration of cisplatin. The cells became rounded and broken when incubated with 10 μg/mL cisplatin, while cell staining with crystalline violet became lighter with increasing concentration (Figure 2.).

Hoechst 33258 staining showed that evident apoptosis of mGC could be observed after 24 h of 5 μg/mL CDDP (Figure 2.). These cells showed nuclear consolidation, nuclear rupture, and nuclear lysis. The formation of apoptotic vesicles could be observed, and a more significant apoptosis was observed with increased cisplatin concentrations (Figure 2.). Altogether, it was shown that 5 μg/mL CDDP for 24 h could dramatically damage mGC while maintaining cell viability to some extent, therefore dose of 5μg/mL CDDP was choose to establish mGC damage model.

ISSN: 2472-3703 DOI: 10.6911/WSRJ.202205_8(5).0066

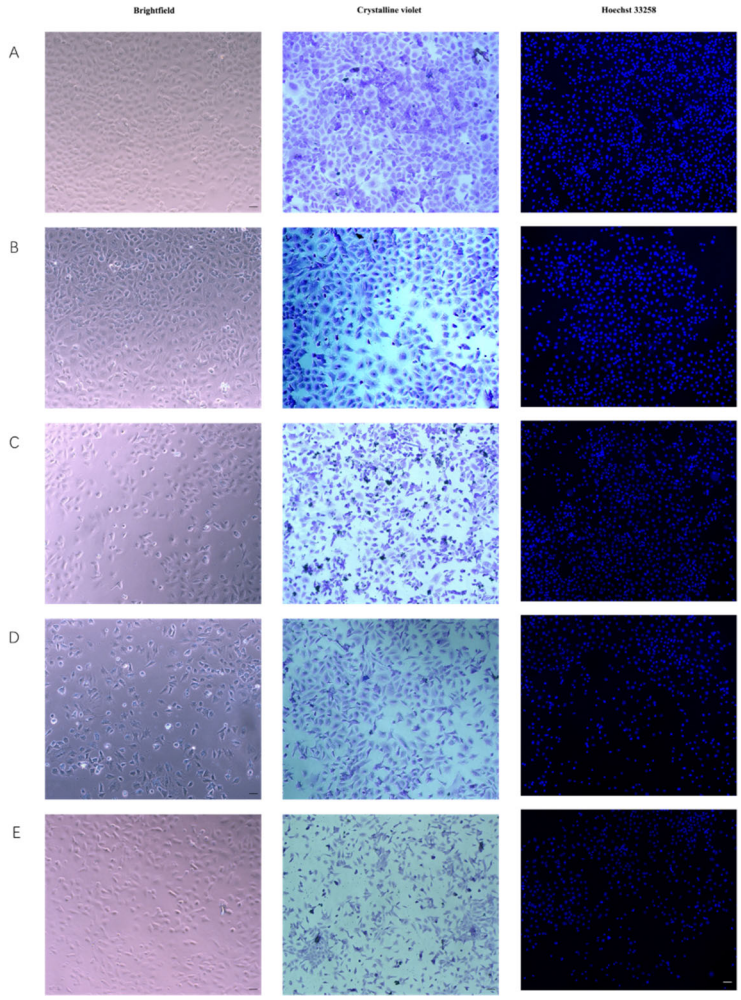

Figure 2. Morphological changes of mGC cells and apoptosis induced by different concentrations of cisplatin (100×).

A: 0 μg/mL CDDP group B: 2.5 μg/mL CDDP group C: 5 μg/mL CDDP group D: 7.5 μg/mL CDDP group E: 10 μg/mL CDDP group with a scale bar of 100 μm.

The growth and cell morphology of mGC cells were observed under light microscopy. mGC could be star-shaped or spindle-shaped, with interconnected cellular pseudopods between cells incontrol(Figure 2.A). Crystalline violet staining could be observed with intact cell morphology and clear edges, and the cells were polygonal, star-shaped, or spindle-shaped. The nuclei were stained dark purple and round by crystalline violet, and lavender stained the cytoplasm. The morphology and physiological staus of isolated cells was were as same a cells in the literature, indicating that the isolated cells were primary mGCs. After cisplatin treatment of different concentrations, the growth condition and morphology of mGC were observed. The results showed that the treatment of 2.5, 5, 7.5, and 10 μg/mL cisplatin significantly inhibited the cell viability of mGC compared with the control group, while there were much fewer cells as the high concentration of cisplatin. The cells became rounded and broken when incubated with 10 μg/mL cisplatin, while cell staining with crystalline violet became lighter with increasing concentration (Figure 2.).

Hoechst 33258 staining showed that evident apoptosis of mGC could be observed after 24 h of 5 μg/mL CDDP (Figure 2.). These cells showed nuclear consolidation, nuclear rupture, and nuclear lysis. The formation of apoptotic vesicles could be observed, and a more significant apoptosis was observed with increased cisplatin concentrations (Figure 2.). Altogether, it was

ISSN: 2472-3703 DOI: 10.6911/WSRJ.202205_8(5).0066

shown that 5 μg/mL CDDP for 24 h could dramatically damage mGC while maintaining cell viability to some extent, therefore dose of 5μg/mL CDDP was choose to establish mGC damage model.

3.2. Effect of FMSC on Cisplatin-induced mGC Damage

3.2.1 Effect of FMSC on the cell proliferation of cisplatin-induced mGC

After establishing the mGC damage model, different concentrations of FMSC were added to investigate the effect of FMSC on CDDP-induced mGC damage.

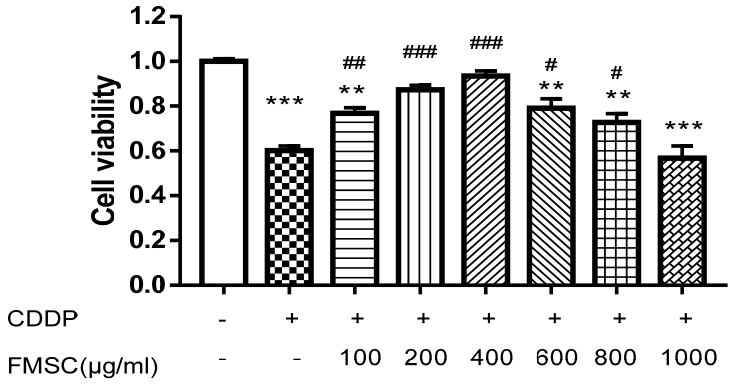

Figure 3. Effect of FMSC on the proliferation of mGCs after cisplatin treatment. **P<0.01, ***P<0.001, compared with the control group; #P<0.05, ##P<0.01, ###P<0.001, compared with the CDDP group.

Table 2. Inhibition rate of mGCs after CDDP treatment by FMSC

Group	Inhibition rate (%)
Control	0 ± 1.15
CDDP (μg/mL)	39.81± 2.00***
CDDP+FMSC 100	23.21 ± 2.50**##
CDDP+FMSC 200	12.66 ± 1.94###
CDDP+FMSC 400	6.61 ± 2.28###
CDDP+FMSC 600	20.87 ± 4.19**#
CDDP+FMSC 800	27.26 ± 3.93**#
CDDP+FMSC 1000	43.17 ± 5.36***

As shown in Figure 3. and Table 2, FMSC preserved/recover mGC cell viability damaged after cisplatin treatment. The results showed that concentrations of 100-800 μg/mL FMSC significantly improved cisplatin-induced cell damage ($P < 0.05$) but did not present a significant dose-response. Meanwhile, the MTT results showed a significant difference in cell viability in the 100-400 μg/mL FMSC concentration groups compared with the cisplatin group ($P < 0.01$). In addition, 400 μg/mL FMSC treated cells showed a cell inhibition rate of 6.61% compared to the control group ($P > 0.05$) and a 32.60% increase in cell viability compared to the cisplatin group.

3.2.2 Effect of FMSC on the cell morphology of cisplatin-damaged mGC

As shown in Figure 4., the number of mGC cells in the CDDP group decreased and the cells became rounded and smaller. Some cells were broken, and cellular debris appeared between cells. The color of crystalline violet staining became lighter than that of the control group, and the intercellular spaces became larger (Figure 4 .B). Cells treated with 100 μg/mL, 200 μg/ mL, and 400 μg/ mL FMSC were protected from the cell damage induced by cisplatin (Figure 4 . B-

ISSN: 2472-3703 DOI: 10.6911/WSRJ.202205_8(5).0066

E), since the number of cells in each FMSC group increased significantly compared with that of the cisplatin group. Cell morphology evidenced the same shuttle or polygonal shape as that of the control group, and the crystalline violet staining showed normal cell morphology in every FMSC-treated group. This effect was dose-dependent.

3.2.3 Effect of FMSC on the apoptosis of cisplatin-damaged mGC cells

In order to investigate whether FMSC exerts its protective effect through inhibiting apoptosis, we examined Hoechst 33258 and TUNEL staining of mGCs. Apoptotic cells were not seen in the control mGC group (Figure 5. A). Compared with the control group, both CDDP and CDDP+FMSC100/200/400 groups had positive apoptotic cells with green fluorescence (Figure 5. B-E, Figure 5. B-E). As shown in Figure 5. B, the CDDP group contained a large amount of bright green fluorescence, and Hoechst 33258 staining showed nuclear sequestration with bright blue fluorescence due to nuclear rupture. In contrast to the CDDP group, there were fewer apoptosis-positive cells in CDDP+ FMSC100/200/400 groups. The results showed that a small number of bright blue apoptotic vesicles and green fluorescent TUNEL positive cells could be observed in the CDDP+FMSCL group when 100 μg/mL FMSC was used. Strong blue apoptotic vesicles and bright green fluorescent TUNEL positive cells were not observed when 400 μg/mL was used.

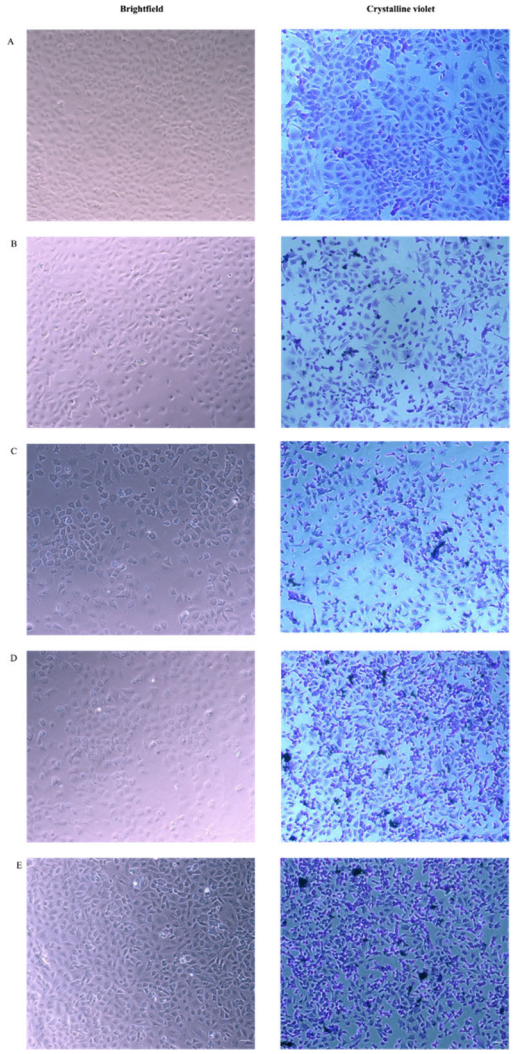

Figure 4. Effect of FMSC on the cell morphology of cisplatin-damaged mGC (100 ×). A: Control group B: CDDP group C: CDDP+FMSC 100 μg/mL group D: CDDP+FMSC 200 μg/mL group E: CDDP+FMSC 400 μg/mL group with a scale bar of 100 μm.

ISSN: 2472-3703 DOI: 10.6911/WSRJ.202205_8(5).0066

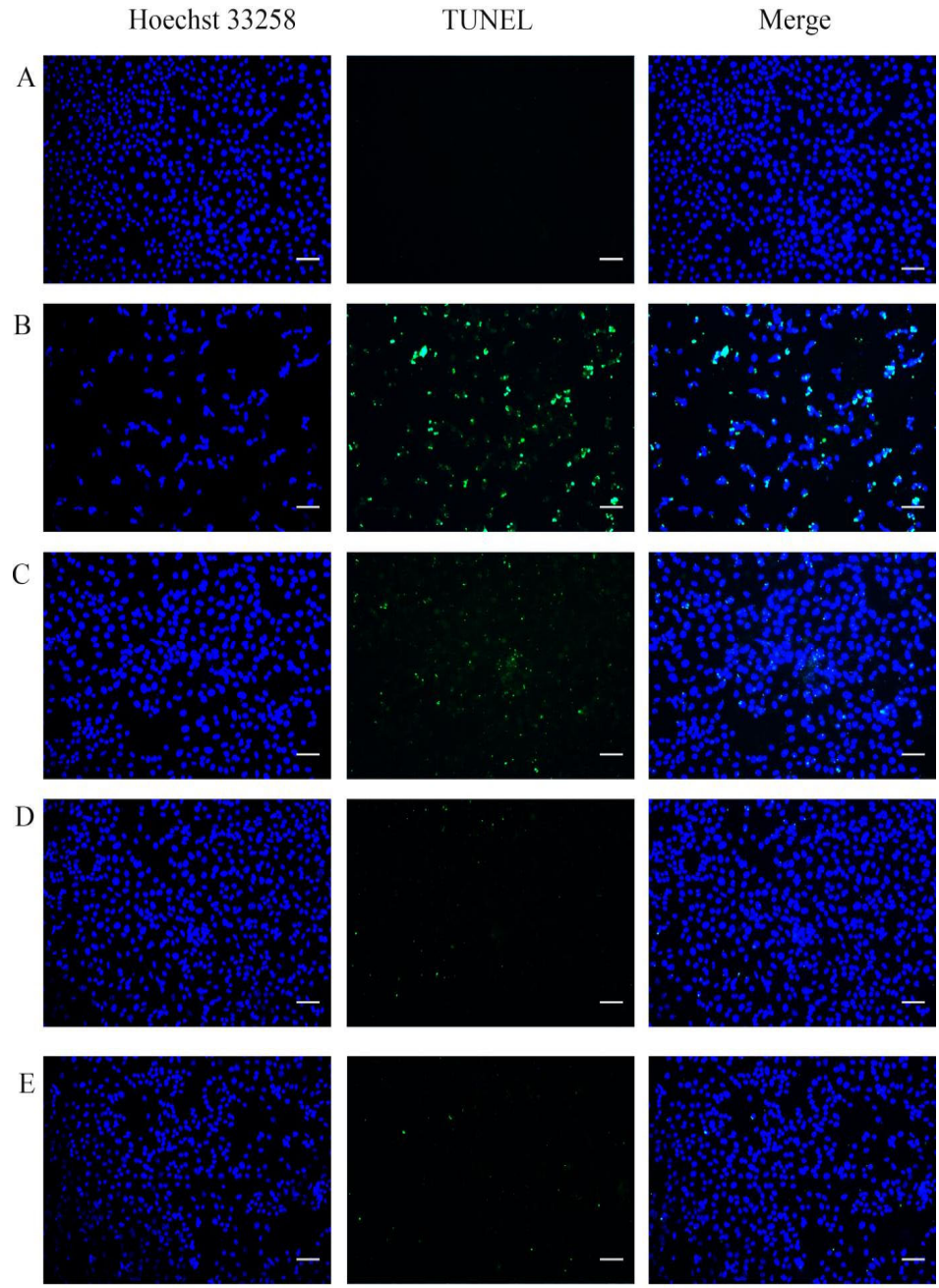

Figure 5. Reversion of apoptosis in cisplatin-damaged mGC by FMSC (100×).
A: Control group B: CDDP group C: CDDP+FMSC 100 μg/mL group D: CDDP+FMSC 200 μg/mL group E: CDDP+FMSC 400 μg/mL group with a scale bar of 100 μm.

3.2.4 Effect of FMSC on apoptosis-related genes Bcl-2 and Bax in cisplatin-damaged mGC

As shown in Figures 4-6, compared with control cells, Bcl-2 decreased by 65.53% ($P < 0.01$) after a 24 hours treatment with 5 μg/mL cisplatin. Treatment with FMSC dose-dependently increased Bcl-2 levels by 74.51% to 186.81% when compared with the cisplatin group ($P < 0.01$). After 24 hours treatment with 5 μg/mL cisplatin, the level of mRNA of the pro-apoptotic gene Bax in mGC was increased by 203.12% compared with that of the control group ($P < 0.01$), and after treatment with FMSC, each group of CDDP+ FMSC100/200/400 showed different degrees of recovery compared with the cisplatin group.

ISSN: 2472-3703 DOI: 10.6911/WSRJ.202205_8(5).0066

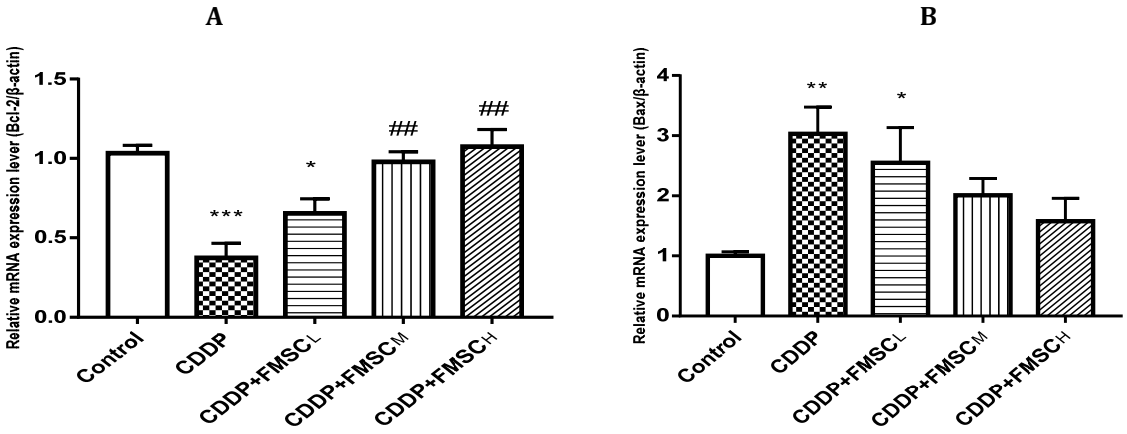

Figure 6. mRNA expression of apoptosis-related genes Bcl-2 and Bax in mGC. A: relative expression of mRNA of Bcl-2; B: relative expression of mRNA of Bax.*P<0.05, **P<0.01, ***P<0.001, compared with the control group; ##P<0.01, compared with the C DDP group.

3.2.5 Effect of FMSC on mGC apoptosis-related proteins Bcl-2, Bax, and proliferation-related protein PCNA

As shown in Figure7., the expression of Bax protein, a pro-apoptotic gene, and PCNA, a proliferative gene, decreased in mGC after 24 hours treatment with 5 μg/mL cisplatin. Compared with the cisplatin group, the protein expression of Bax decreased, while Bcl-2 and PCNA protein levels were upregulated in cells treated with FMSC.

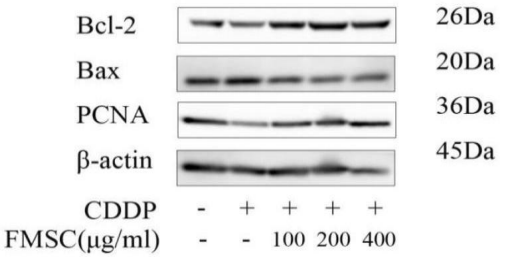

Figure 7. Expression of apoptosis-related proteins Bcl-2 and Bax, and proliferation-related protein PCNA in mGCs.

4. DISCUSSION

Granulosa cells are a major component of the ovary and play avital role for ovarian function while the ovarian follicle is the basic structural and functional unit of this organ. The ovarian follicle is composed of the oocyte, located in the core?, and the surrounding granulosa and membrane cells. Granulosa cell proliferation and differentiation play a crucial role in ovarian functions, included normal growth and development, proliferation, differentiation, atresia, and ovulation. Resarchs [29,30,31,32] showed that cisplatin could induce apoptosis of ovarian and granulosa cells, disturbance of hormone levels, and ovarian failure, which leads to ovarian damage. Ovarian estrogens and progesterone are essential steroid hormones for the development of female reproductive system. The hypothalamus-pituitary-gonads axis regulates the secretion of hormones from the ovary. The anterior pituitary gland secretes the stimulating follicle hormone FSH. Granulosa cells, the only cells with expression the FSH receptor (FSHR), sense FSH and promote the secretion of estrogen to function at the late stage of follicular

ISSN: 2472-3703 DOI: 10.6911/WSRJ.202205_8(5).0066

development. Current studies showed that FSHR knockout in female mice have impaired follicle development, lower estrogen levels and cause ovarian atrophy in comparion with normal developed mice. Anti-Müllerian hormone secreted by Granulosa cells of growing follicles, a regulatory protein of primordial follicle activation, inhibits the recruitment and growth of primordial follicles. In addition, granulosa cells also serve as progesterone and estrogen synthesis sites, the synthsis changes of hormone regulated by steroid-related proteins expressed in granulosa cells are key to cholesterol uptake, synthesis, and transport, as in the processing of cholesterol to progesterone and estrogen. The proteins associated with progesterone and estrogen synthesis include steroid hormone synthesis acute regulatory protein (StAR), cholesterol side-chain cleavage enzymes (P450scc/CYP11A1), cytochrome P450 enzyme 17A1 (CYP17A1), cytochrome P450 enzyme 19A1 (CYP19A1), 3β-hydroxysteroid dehydrogenase (3β-HSD), 17β -hydroxysteroid dehydrogenase (17β-HSD) and others [33]. Therefore, granulosa cell proliferation, differentiation, and FSHR expression are crucial for the ovaries to exert their physiological functions.

In this study, mGCs were isolated and established cell damage model in vitro with cisplatin treatment. Intervention with FMSC was performed to investigate the effect of FMSC on damage of ovarian granulosa cells and underlying mechanisms. Cell proliferation was detected by the MTT assay, cell growth was observed using crystal violet, and apoptosis was assessed by TUNEL & Hoechst 33258 staining. qPCR and Western Blot (WB) were performed to respectively measure mRNA and protein expression of proliferation-related molecules (PCNA) and apoptosis-related molecules (Bax and Bcl-2).

Upon exposure to cisplatin, the cell inhibition rate was 34.12% in the MTT assay after 24 h of mGC treatment with 5 μg/mL cisplatin compared with that of the control group. In addition, changes in cell morphology were observed by crystalline violet and Hoechst stainings, which evidenced round cells, wrinkling, nuclear consolidation, and apoptotic vesicles after 24 h of exposure to 5 μg/mL cisplatin. Therefore, 5 μg/mL cisplatin was chosen as our cisplatin-damaged model.

As a traditional Chinese medicine, the effect of FMSC on cisplatin-induced granulosa cell damage was experimentally explored. The experimental results showed that FMSC at concentrations of 100-400 μg/mL had a significant protective effect on cisplatin-induced granulocyte damage. After FMSC treatment, the inhibition rate of mGC cells in the group treated with 400 μg/mL FMSC was 6.61% compared with that of the control group ($P>0.05$), and the cell viability was enhanced by 55.12% compared with that of the cisplatin group. The inhibition rate of KGN cells treated with CDDP and 400 μg/mL FMSC was 8.97% compared with the control group ($P> 0.05$), and the cell viability was increased by 35.72% compared to the cisplatin group. In addition, crystalline violet staining showed that FMSC significantly improved granulosa cell injury induced by CDDP. Mechanistically, FMSC could reduce the mRNA and protein expressions of Bax, a pro-apoptotic gene, which was induced by cisplatin. Meanwhile, the expression of apoptosis-suppressing gene Bcl-2 and cell proliferation gene PCNA were significantly upregulated in cells exposed to FMSC when compared with the cisplatin group.

ACKNOWLEDGMENTS

This work is supported by grants from the Forestry Science and Technology Innovation Project of Guangdong Province (Project number: 2021KJCX013).

REFERENCES

[1] Achkar I W, Abdulrahman N, Al-Sulaiti H, et al. 2018. Cisplatin based therapy: the role of the mitogen activated protein kinase signaling pathway[J]. Journal of Translational Medicine, 2018, 16(1): 96..

ISSN: 2472-3703 DOI: 10.6911/WSRJ.202205_8(5).0066

[2] Ali A, Burak Z, Levent A, et al. 2014. Granulocyte-colony stimulating factor decreases the extent of ovarian damage caused by cisplatin in an experimental rat model[J]. Journal of gynecologic oncology, 25(4).328

[3] Arab H H, Mohamed W R, Barakat B M, et al. 2016. Tangeretin attenuates cisplatin-induced renal injury in rats: Impact on the inflammatory cascade and oxidative perturbations[J]. Chemico-biological interactions, 258: 205-213.

[4] Neamatallah T, El-Shitany N A, Abbas A T, et al. 2018. Honey protects against cisplatin-induced hepatic and renal toxicity through inhibition of NF-κB-mediated COX-2 expression and the oxidative stress dependent BAX/Bcl-2/caspase-3 apoptotic pathway[J]. Food & function, 9(7): 3743-3754.

[5] Lebwohl D, Canetta R. 1998. Clinical development of platinum complexes in cancer therapy: an historical perspective and an update[J]. European journal of cancer, 34(10): 1522-1534.

[6] Kelland L. 2007. The resurgence of platinum-based cancer chemotherapy[J]. Nature Reviews Cancer, 7(8): 573-584.

[7] Yanyan Y, Ogun A, Gang W, et al. 2018. Cisplatin-DNA adduct repair of transcribed genes is controlled by two circadian programs in mouse tissues[J]. Proceedings of the National Academy of Sciences of the United States of America, 2018, 115(21): E4777-E4785

[8] Yang H, Qiong-Ni Z, Jun-Li D, et al. 2018. Emerging role of long non-coding RNAs in cisplatin resistance[J]. OncoTargets and therapy, 2018, 11: 3185.

[9] Ishida S, Lee J, Thiele D J, et al. 2002. Uptake of the Anticancer Drug Cisplatin Mediated by the Copper Transporter Ctr1 in Yeast and Mammals[J]. Proceedings of the National Academy of Sciences of the United States of America, 2002, 99(22): 14298-14302.

[10] Alan E. 1987. The formation, isolation and characterization of DNA adducts produced by anticancer platinum complexes[J]. Pergamon, 1987, 34(2): 155-166.

[11] Tope C A. 2015. Relative Reaction Rates of the Amino Acids Cysteine, Methionine, and Histidine with Analogs of the Anti-Cancer Drug Cisplatin[J].2015: 571.

[12] Marullo R, Werner E, Degtyareva N, et al. 2013. Cisplatin Induces a Mitochondrial-ROS Response That Contributes to Cytotoxicity Depending on Mitochondrial Redox Status and Bioenergetic Functions[J]. Plos One, 8(11).

[13] Guerrero-Beltrán C E, Calderón-Oliver M, Martínez-Abundis E, et al. 2010. Protective effect of sulforaphane against cisplatin-induced mitochondrial alterations and impairment in the activity of NAD (P) H: quinone oxidoreductase 1 and γ glutamyl cysteine ligase: studies in mitochondria isolated from rat kidney and in LLC-PK1 cells[J]. Toxicology letters, 199(1): 80-92.

[14] Y S S, O N T A, Mouied A. 2004. Role of non-selective adenosine receptor blockade and phosphodiesterase inhibition in cisplatin-induced nephrogonadal toxicity in rats[J]. Clinical and experimental pharmacology & physiology, 2004, 31(12): 862-867.

[15] Rodrigues M C, Rodrigues J, Martins N, et al. 2011. Carvedilol protects against cisplatin-induced oxidative stress, redox state unbalance and apoptosis in rat kidney mitochondria[J]. Chemico-biological interactions, 189(1-2): 45-51.

[16] Chirino Y I, Trujillo J, Sánchez-González D J, et al. 2008. Selective iNOS inhibition reduces renal damage induced by cisplatin[J]. Toxicology letters, 176(1): 48-57.

[17] Green D R. 1998. Apoptotic pathways: the roads to ruin[J]. Cell, 94(6): 695-698.

[18] Fuertes M A, Alonso C, Pérez J M. 2003. Biochemical modulation of cisplatin mechanisms of action: enhancement of antitumor activity and circumvention of drug resistance[J]. Chemical reviews, 103(3): 645-662.

ISSN: 2472-3703 DOI: 10.6911/WSRJ.202205_8(5).0066

[19] Lorenzo G, Eugenia M, Oliver K, et al. 2011. Mitochondrial liaisons of p53[J]. Antioxidants & redox signaling, 2011, 15(6): 1691-1714.

[20] Hummitzsch K, Anderson RA, Wilhelm D, Wu J, Telfer EE, Russell DL, et al. Stem cells, progenitor cells, and lineage decisions in the ovary. Endocr Rev. (2015) 36:65–91. doi: 10.1210/er.2014-1079

[21] Thomas FH, Vanderhyden BC. Oocyte-granulosa cell interactions during mouse follicular development: regulation of kit ligand expression and its role in oocyte growth. Reprod Biol Endocrinol. (2006) 4:1–8. doi: 10.1186/1477-7827-4-1

[22] Aerts JMJ, Bols PEJ. Ovarian follicular dynamics: a review with emphasis on the bovine species. Part I: folliculogenesis and pre- antral follicle development. Reprod Domest Anim. (2010) 45:171–9. doi: 10.1111/j.1439-0531.2008.01302.x

[23] Jang H, Na Y, Hong K, et al. 2017. Synergistic effect of melatonin and ghrelin in preventing cisplatin-induced ovarian damage via regulation of FOXO 3a phosphorylation and binding to the p27Kip1 promoter in primordial follicles[J]. Journal of Pineal Research, 63(3): e12432.

[24] Wu Y, Ma C, Zhao H, et al. 2018. Alleviation of endoplasmic reticulum stress protects against cisplatin-induced ovarian damage[J]. Reproductive Biology and Endocrinology, 16(1): 1-12.

[25] Said R S, Mantawy E M, El-Demerdash E. 2019. Mechanistic perspective of protective effects of resveratrol against cisplatin-induced ovarian injury in rats: emphasis on anti-inflammatory and anti-apoptotic effects[J]. Naunyn-Schmiedebergs Archives of Pharmacology, 392(10): 1225-1238.

[26] Wang J, Ruan W, Huang B, et al. Tri-ortho-cresyl phosphate induces autophagy of mouse ovarian granulosa cells. Reproduction. 2019;158: 61-69.

[27] Canipari R, O'Connell ML, Meyer G, Strickland S. Mouse ovarian gran- ulosa cells produce urokinase-type plasminogen activator, whereas the corresponding rat cells produce tissue-type plasminogen activa- tor. J Cell Biol. 1987;105(2):977-981.

[28] Huang J, Shan W, Li N, et al. 2021. Melatonin provides protection against cisplatin-induced ovarian damage and loss of fertility in mice[J]. Reproductive biomedicine online, 42(3): 505-519.

[29] Zhang J, Yin H, Jiang H, et al. 2020. The protective effects of human umbilical cord mesenchymal stem cell-derived extracellular vesicles on cisplatin-damaged granulosa cells[J]. Taiwanese Journal of Obstetrics & Gynecology, 59(4): 527-533.

[30] Xie Y, Li S, Zhou L, et al. 2020. Rapamycin preserves the primordial follicle pool during cisplatin treatment in vitro and in vivo[J]. Molecular reproduction and development, 87(4): 442-453.

[31] Ibrahim M A, Albahlol I A, Wani F A, et al. 2021. Resveratrol Protects against Cisplatin-induced Ovarian and Uterine Toxicity in Female Rats by Attenuating Oxidative Stress, Inflammation and Apoptosis[J]. Chemico-biological interactions: 109402-109402.

[32] Hu J, Zhang Z, Shen W-J, et al. 2010. Cellular cholesterol delivery, intracellular processing and utilization for biosynthesis of steroid hormones[J]. Nutrition & metabolism, 7(1): 1-25.